AD-A077 640 VERMONT UNIV BURLINGTON DEPT OF CHEMISTRY F/G 7/3
APPLICATIONS OF THE MOESSBAUER EFFECT TO THE STUDY OF MIXED-VAL--ETC(U)
NOV 79 D B BROWN , J T WROBLESKI N00014-75-C-0756
UNCLASSIFIED TR-19 NL

| OF |
ADA
077640

END
DATE
FILMED
1 -80
DDC

LEVEL II

12 B.S.

OFFICE OF NAVAL RESEARCH

(15) Contract N00014-75-C-0756

Task No. NR 356-593

(9) TECHNICAL REPORT NO. 19 (14) TR-1

(6) Applications of the Mössbauer Effect to the Study of Mixed-Valence Compounds,

by

(10) David B. Brown and James T. Wrobleski



Prepared for publication in

"Mixed-Valence Compounds", D. B. Brown, ed.

D. Reidel Publishing Company (1980).

(11) 26 November 1979 (12) 31

SECURITY CLASSIFICATION OF THIS PAGE (When Data Entered)

| REPORT DOCUMENTATION PAGE | | READ INSTRUCTIONS BEFORE COMPLETING FORM |
|---|---|---|
| 1. REPORT NUMBER<br>19 | 2. GOVT ACCESSION NO. | 3. RECIPIENT'S CATALOG NUMBER |
| 4. TITLE (and Subtitle)<br>"Applications of the Mössbauer Effect to the Study of Mixed-Valence Compounds" | | 5. TYPE OF REPORT & PERIOD COVERED<br>Technical Report<br>6. PERFORMING ORG. REPORT NUMBER |
| 7. AUTHOR(s)<br>David B. Brown and James T. Wrobleski | | 8. CONTRACT OR GRANT NUMBER(s)<br>N00014-75-C-0756 |
| 9. PERFORMING ORGANIZATION NAME AND ADDRESS<br>Department of Chemistry<br>University of Vermont<br>Burlington, Vermont 05405 | | 10. PROGRAM ELEMENT, PROJECT, TASK AREA & WORK UNIT NUMBERS |
| 11. CONTROLLING OFFICE NAME AND ADDRESS<br>Office of Naval Research<br>Department of the Navy<br>Arlington, Virginia 22217 | | 12. REPORT DATE<br>November 26, 1979<br>13. NUMBER OF PAGES<br>28 |
| 14. MONITORING AGENCY NAME & ADDRESS(if different from Controlling Office) | | 15. SECURITY CLASS. (of this report)<br>Unclassified<br>15a. DECLASSIFICATION/DOWNGRADING SCHEDULE |

16. DISTRIBUTION STATEMENT (of this Report)

This document has been approved for public release and sale; its distribution is unlimited.

17. DISTRIBUTION STATEMENT (of the abstract entered in Block 20, if different from Report)

18. SUPPLEMENTARY NOTES

Prepared for publication in "Mixed-Valence Compounds," D. B. Brown, editor.

19. KEY WORDS (Continue on reverse side if necessary and identify by block number)

γ-ray resonance, isomer shifts, quadrupole splittings, hyperfine interactions, valence interchange, relaxation

20. ABSTRACT (Continue on reverse side if necessary and identify by block number)

The principal utility of Mössbauer Effect spectroscopy in the study of mixed-valence materials is its ability (through measurement of the chemical shift) to distinguish between different oxidation states of the same element in similar chemical environments. By using Mössbauer Effect spectroscopy it is possible to distinguish between trapped and delocalized valence states in mixed-valence compounds. In addition, the rather long lifetime of the Mössbauer experiment, as compared to other forms of spectroscopy, permits evaluation of the rate of intervalence electron exchange in mixed-valence materials.

DD FORM 1 JAN 73 1473 EDITION OF 1 NOV 63 IS OBSOLETE
S/N 0102-014-6601

SECURITY CLASSIFICATION OF THIS PAGE (When Data Entered)

# APPLICATIONS OF THE MÖSSBAUER EFFECT TO THE STUDY OF MIXED-VALENCE COMPOUNDS

David E. Brown and James T. Wrobleski*

Department of Chemistry, University of Vermont,
Burlington, Vermont 05405

## Abstract

The principal utility of Mössbauer Effect spectroscopy in the study of mixed-valence materials is its ability (through measurement of the chemical isomer shift) to distinguish between different oxidation states of the same element in similar chemical environments. By using Mössbauer Effect spectroscopy it is possible to distinguish between trapped and delocalized valence states in mixed-valence compounds. In addition, the rather long lifetime of the Mössbauer experiment, as compared to other forms of spectroscopy, permits evaluation of the rate of intervalence electron exchange in mixed-valence materials.

## INTRODUCTION

In recent years the Mössbauer Effect (ME), a form of nuclear $\gamma$-ray resonance spectroscopy, has been applied to a broad range of research problems involving mixed-valence materials. As a result, our understanding of the role of mixed valency in certain areas of catalysis, corrosion science, biological redox reactions, mineralogy, and the study of impurity structures in semiconductors and metals has progressed substantially.

ME spectroscopy is a powerful tool for the study of mixed-valence materials because it can distinguish different oxidation states of the same element in similar chemical environments. Through application of the ME one may obtain information about

*Present address: Monsanto Co., St. Louis, Missouri.

both structural and magnetic properties of mixed-valence compounds. In certain cases it is also possible to probe dynamic features of the mixed-valence state such as kinetics of intervalence electron transfer in semiconductors and isolated metal ion clusters.

The purpose of this article is to illustrate the types of research problem involving mixed-valence compounds which have been examined with ME spectroscopy. Experimental results which demonstrate the applicability of ME spectroscopy to mixed-valence materials are preceded by a brief, operational introduction to the ME. Those readers who wish more detailed discussion of the ME are encouraged to consult works listed in the general references list at the end of this paper.



## DESCRIPTION OF THE MÖSSBAUER EFFECT

The fundamental nuclear event which describes ME spectroscopy is the recoilless (zero-phonon) emission or absorption of a $\gamma$ ray. In the usual ME experiment (Figure 1a) a radioactive parent nuclide decays to a daughter (the source) with excited state $|\psi_e^S\rangle$ and nuclear half life $\tau_n$. A fraction $\underline{f}$ of the excited state nuclei decay to the ground state $|\psi_g^S\rangle$ with emission of a $\gamma$ ray $\gamma_M$ which has not suffered energy loss due to recoil effects. This recoilless fraction $\underline{f}$ is a function of both the energy of $\gamma_M$ and the lattice dynamics of the source material. When the source is brought in the vicinity of a material (the absorber) whose nuclear energy levels exactly match its own, $\gamma_M$ may be resonantly absorbed

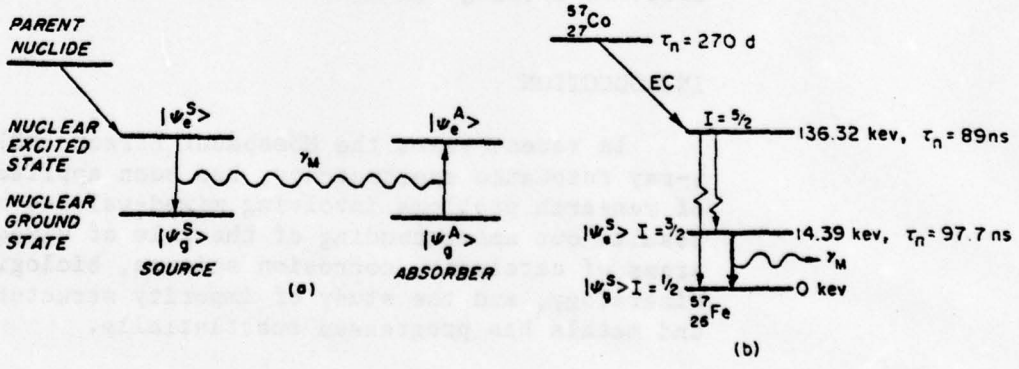


Figure 1. Schematic illustrations of nuclear processes important in ME spectroscopy. (a) Recoilless emission + absorption of ME gamma ray, $\gamma_M$. (b) Specific decay scheme for $^{57}_{27}Co$ decay to $^{57}_{26}Fe$ with production of 14.4 keV $\gamma_M$.

# APPLICATIONS OF THE MÖSSBAUER EFFECT TO THE STUDY OF MIXED-VALENCE COMPOUNDS

David B. Brown and James T. Wrobleski*

Department of Chemistry, University of Vermont, Burlington, Vermont 05405

## Abstract

The principal utility of Mössbauer Effect spectroscopy in the study of mixed-valence materials is its ability (through measurement of the chemical isomer shift) to distinguish between different oxidation states of the same element in similar chemical environments. By using Mössbauer Effect spectroscopy it is possible to distinguish between trapped and delocalized valence states in mixed-valence compounds. In addition, the rather long lifetime of the Mössbauer experiment, as compared to other forms of spectroscopy, permits evaluation of the rate of intervalence electron exchange in mixed-valence materials.

## INTRODUCTION

In recent years the Mössbauer Effect (ME), a form of nuclear $\gamma$-ray resonance spectroscopy, has been applied to a broad range of research problems involving mixed-valence materials. As a result, our understanding of the role of mixed valency in certain areas of catalysis, corrosion science, biological redox reactions, mineralogy, and the study of impurity structures in semiconductors and metals has progressed substantially.

ME spectroscopy is a powerful tool for the study of mixed-valence materials because it can distinguish different oxidation states of the same element in similar chemical environments. Through application of the ME one may obtain information about

*Present address: Monsanto Co., St. Louis, Missouri.

to populate a nuclear excited state $|\psi_e^A\rangle$ in the absorber. Figure 1b illustrates the decay scheme of $^{57}Co$ which is used to populate the nuclear excited state of $^{57}Fe$, the most widely-studied ME nuclide.

Two types of source + absorber geometries are commonly employed in ME spectroscopy. These geometries are illustrated in Figure 2. In transmission geometry (Figure 2a) the absorber is positioned between source and detector and the $\gamma$ ray energy distribution transmitted through the absorber is recorded. A sketch in the lower portion of Figure 2a represents a spectrum which is obtained in this manner. In the backscatter experiment (Figure 2b) the detector and source are shielded from one another on the same side of the absorber (scatterer) and the detector records the energy distribution of resonant fluorescence emitted from $|\psi_e^A\rangle$.

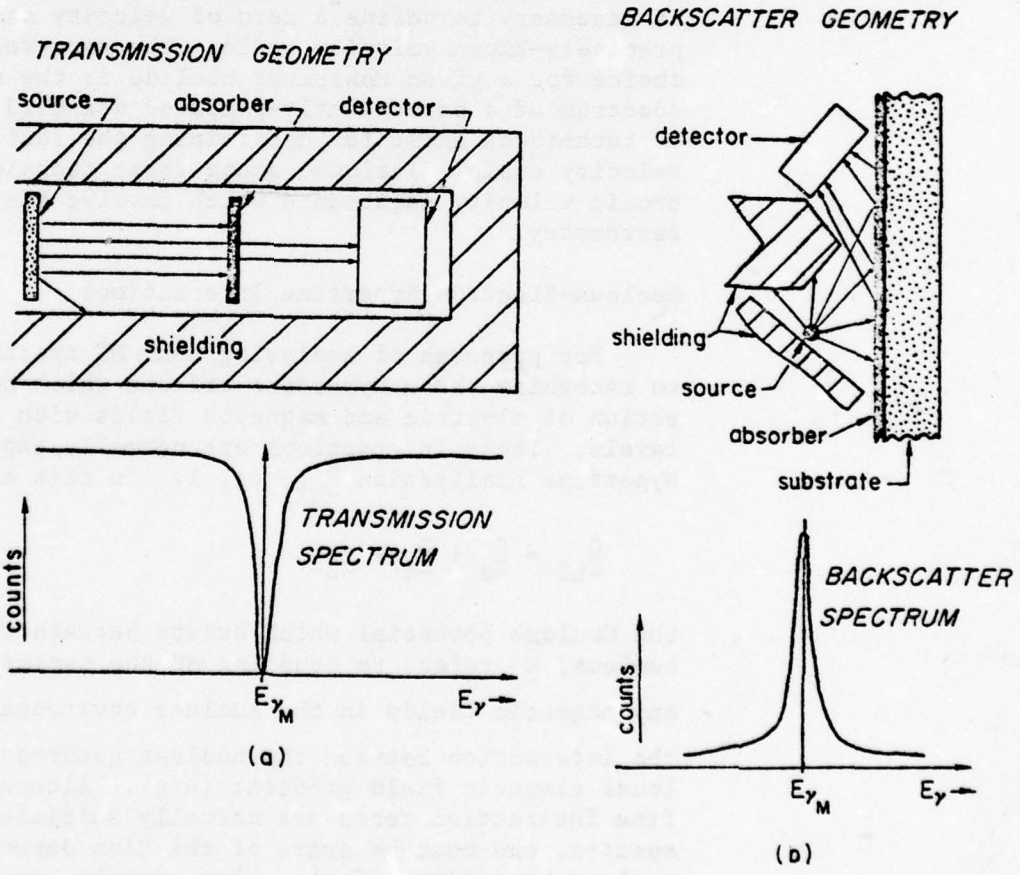


Figure 2. The two types of source + absorber ME experimental geometries. (a) Transmission geometry. (b) Backscatter geometry.

A spectrum obtained in the backsactter geometry is illustrated in the lower portion of Figure 2b.

In the experiments described above it is apparent that if the absorber nuclear ground-excited state splitting does not exactly match the energy of $\gamma_M$ the system is off resonance: that is, no $\gamma$ ray absorption will occur. In order to bring the system into resonance it is necessary to move the source or absorber. This relative motion modulates the energy of $\gamma_M$ by an amount $\underline{E}'(\underline{v})$ dictated by the Doppler effect [$\underline{E}'(\underline{v}) = \pm(\underline{v}/\underline{c})\underline{E}_{\gamma_M}$], where $\underline{v}$ is the relative velocity of source with respect to absorber, $\underline{c}$ is the speed of light, and $\underline{E}_{\gamma_M}$ is the energy of the unmodulated Mössbauer $\gamma$ ray. By convention the positive sign in this Doppler equation refers to closing velocities. Because the nuclear energy shifts of importance in the ME are of the order $1 \times 10^{-3}$ $cm^{-1}$, it is seldom necessary for $|\underline{v}|$ to exceed 10 or 20 mm/sec. However, it is necessary to define a zero of velocity and have available a precisely-known velocity scale. The zero-velocity calibrant of choice for a given Mössbauer nuclide is the centroid of the ME spectrum of a conveniently-prepared standard absorber. A variety of techniques exist for determining the functional form of the velocity scale. Included among these techniques are purely electronic velocity calibrants which involve the use of Moiré interferrometry.

Nucleus-Electron Hyperfine Interactions

For purposes of analyzing most ME spectra it is sufficient to recognize three hyperfine effects which result from the interaction of electric and magnetic fields with the nuclear energy levels. These interactions are normally expressed in terms of a hyperfine hamiltonian $\hat{\underline{H}}_{hf}$, eq. 1. In this equation $\hat{\underline{E}}_o$ represents

$$\hat{\underline{H}}_{hf} = \hat{\underline{E}}_o + \hat{\underline{M}}_1 + \hat{\underline{E}}_2 \qquad (1)$$

the Coulomb potential which exists between the electrons and nucleus, $\hat{\underline{M}}_1$ refers to coupling of the nuclear magnetic moment with any magnetic fields in the nuclear environment, and $\hat{\underline{E}}_2$ describes the interaction between the nuclear quadrupole moment and the local electric field gradient (efg). Although these three hyperfine interaction terms are normally sufficient to describe ME spectra, one must be aware of the time dependence of electron-nuclear hyperfine effects. For example, one should anticipate complicated spectra when local efg's and magnetic fields are fluctuating at a rate comparable to the Mössbauer excited state relaxation rate $\underline{k}_n(\equiv 1/\tau_n)$. In these instances it is necessary to compute

the time dependent part of $\hat{H}_{hf}$ by assuming a suitable relaxation model. In the area of mixed-valence materials these complicating features are encountered when, for instance, the intervalence electron transfer rate $k_e$ is of order $k_n$.

Coulomb Interactions (Isomer Shift)

In most chemical applications it is convenient and permissible to a high degree of accuracy to treat electronic and nuclear properties as separable (the Born-Oppenheimer approximation). This assumption implies that nuclear energy levels are insignificantly perturbed by their electronic environment. The ME, however, is capable of detecting the minute energy shifts which arise from nucleus-electron coupling. For example, the Coulomb interaction between the nuclear energy levels and their electronic environment depends upon the penetration of electron density into the finite nuclear volume. Because s electrons have a finite probability of existing at the nucleus, the Coulomb interaction depends on the s electron probability density at the nucleus $|\Psi_s(o)|^2$. In addition, because the rms nuclear radius changes by an amount $\delta R$ upon emission or absorption of a $\gamma$ ray, the Coulomb interaction between the nucleus and its environment changes by an amount $\Delta w$ which is given by eq. 2.

$$\Delta w = \text{constant} \times \delta R \times |\Psi_s(o)|^2 \qquad (2)$$

In a ME source + absorber experiment one measures the difference between $\Delta w$ for the source and $\Delta w$ for the absorber. This difference is called the isomer shift $\delta$ and is given by eq. 3.

$$\delta = \text{constant} \times \delta R\{|\Psi_s^A(o)|^2 - |\Psi_s^S(o)|^2\} \qquad (3)$$

It is thus evident that measurement of the Mössbauer isomer shift will provide information about the electronic (chemical) environment in which the nucleus resides. The importance of $\delta$ for study of mixed-valence compounds is nicely illustrated by considering the range of $\delta$ values given in Table I for some commonly-encountered oxidation states of Mössbauer nuclei. For elements in which $\delta R$ is positive, a decrease in the number of p or d electrons increases $\delta$ because of decreased shielding of the s electrons from the nucleus. Conversely, for $^{57}Fe$, in which $\delta R$ is negative, a decrease in 3d electron density results in a decrease in the isomer shift.

Quadrupole Interactions (Quadrupole Splitting)

Nuclear states with spin quantum number I greater than 1/2 possess non-zero quadrupole moments Q and therefore may be split

Table I

Average Isomer Shift Values of Selected Mössbauer Nuclides

| Mössbauer Nuclide | Formal Oxidation State | Formal Electron Configuration | Average δ, mm/s |
|---|---|---|---|
| $^{57}Fe$[a] | $Fe^{2+}$ | $[Ar]4s^0 3d^6$ | 1.0 |
| (-δR) | $Fe^{3+}$ | $[Ar]4s^0 3d^5$ | 0.4 |
| | $Fe^{4+}$ | $[Ar]4s^0 3d^4$ | 0.0 |
| | $Fe^{6+}$ | $[Ar]4s^0 3d^2$ | - 0.8 |
| $^{99}Ru$[b] | $Ru^{2+}$ | $[Kr]5s^0 4d^6$ | - 0.7 |
| (+δR) | $Ru^{3+}$ | $[Kr]5s^0 4d^5$ | - 0.5 |
| | $Ru^{4+}$ | $[Kr]5s^0 4d^4$ | - 0.3 |
| | $Ru^{6+}$ | $[Kr]5s^0 4d^2$ | 0.4 |
| | $Ru^{7+}$ | $[Kr]5s^0 4d^1$ | 0.8 |
| | $Ru^{8+}$ | $[Kr]5s^0 4d^0$ | 1.0 |
| $^{119}Sn$[c] | $Sn^{2+}$ | $[Kr]4d^{10} 5s^0 5p^2$ | > 2.9 |
| (+δR) | $Sn^{4+}$ | $[Kr]4d^{10} 5s^0 5p^0$ | < 2.0 |
| $^{151}Eu$[d] | $Eu^{2+}$ | $[Xe]6s^0 4f^7$ | -13.0 |
| (+δR)? | $Eu^{3+}$ | $[Xe]6s^0 4f^6$ | 0.0 |

δ relative to: [a] Fe metal, [b] Ru metal, [c] $SnO_2$, and [d] $Eu_2O_3$.

by interaction with a finite efg. In any principal axis system the efg tensor is diagonal and traceless. If the three diagonal elements of the efg tensor are $\underline{V}_{xx}$, $\underline{V}_{yy}$, and $\underline{V}_{zz}$ and if $|\underline{V}_{zz}| = \underline{eq}$ is the largest element then $\hat{\underline{E}}_2$ in eq. 1 is given by eq. 4,

$$\hat{\underline{E}}_2 = \underline{e}^2\underline{qQ}[3\hat{\underline{I}}_z^2 - \underline{I}(\underline{I}+1) + \eta(\hat{\underline{I}}_x^2 - \hat{\underline{I}}_y^2)]/4\underline{I}(2\underline{I}-1) \qquad (4)$$

where $\hat{\underline{I}}_x$, $\hat{\underline{I}}_y$, and $\hat{\underline{I}}_z$ are spin operators and $\eta = (\underline{V}_{xx} - \underline{V}_{yy})/\underline{V}_{zz}$, the asymmetry parameter, indicates the degree of asymmetry of the efg tensor. Thus $\eta = 0$ implies an axially-symmetric efg while $0 < \eta \leq 1$ is indicative of an efg with less than axial symmetry.

In materials containing, for example, $^{57}$Fe, $^{119}$Sn, $^{193}$Ir, or $^{195}$Pt ME transitions may be observed between nuclear spin levels 1/2 and 3/2 (written as 1/2↔3/2). For $^{99}$Ru 3/2↔5/2 transitions are observed and for $^{151}$Eu 5/2↔7/2 transitions are possible. The effect of quadrupole coupling with each of these level systems is shown in Figure 3 for a positive $\underline{V}_{zz}$. If $\underline{V}_{zz}$ is negative both excited and ground state splittings are inverted. Numbers given in the circles which accompany each transition indicate the relative transition probability for randomally-oriented polycrystalline samples. In the case of 1/2↔3/2 quadrupole-split spectra the separation between individual transitions of the quadrupole doublet is referred to as the quadrupole splitting and is numerically equal to $1/2\underline{e}^2\underline{qQ}(1 + \eta^2/3)^{1/2}[\equiv 1/2\underline{eQV}_{zz}(1 + \eta^2/3)^{1/2}]$. The quadrupole splitting is given the symbol $\Delta$ (some authors prefer $\Delta\underline{E}_Q$). Examination of the quadrupole spectra for the 3/2↔5/2 and 5/2↔7/2 systems allows a determination of both the sign and magnitude of $\underline{V}_{zz}$. However, because the 1/2↔3/2 quadrupole splitting is symmetric, quadrupole-split ME spectra of these systems provide only the absolute value of $\Delta$.

The quadrupole-split spectrum for a compound with a 1/2↔3/2 nucleus, $^{57}Fe(C_2O_4)(H_2O)_2$, is compared in Figure 4 with a more complicated quadrupole spectrum for $^{129}I_2$ which is a 5/2↔7/2 spin system.

Although it is very difficult to calculate $\Delta$ from principles of bonding theory, a knowledge of the magnitude, sign, and temperature dependence of $\Delta$ is important in any qualitative picture of the electronic structure and chemical bonding in the material of interest. This is particularly true for $^{57}$Fe-containing materials for which an enormous number of ME spectra have been obtained

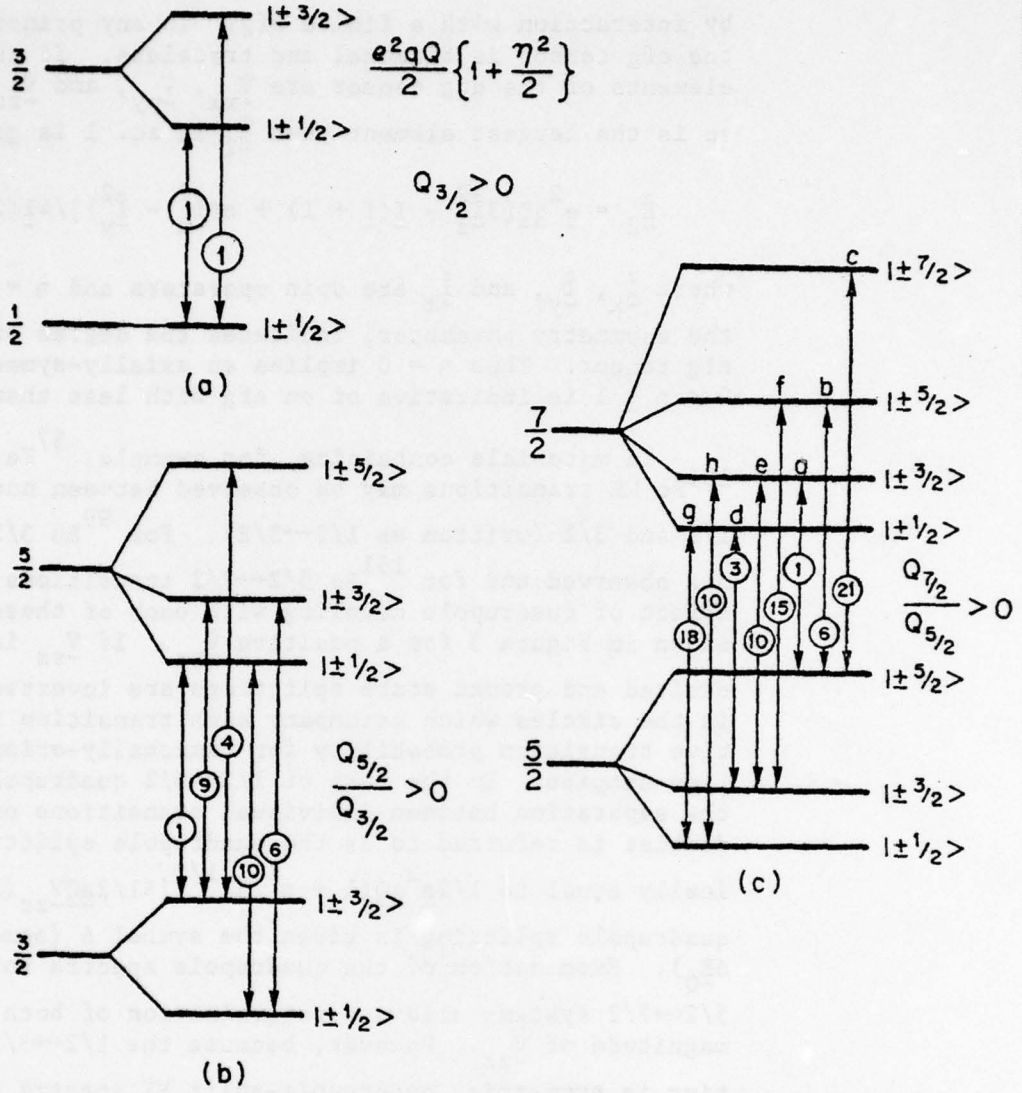


Figure 3. Quadrupole splitting of nuclear spin levels for (a) 1/2↔3/2, (b) 3/2↔5/2, and (c) 5/2↔7/2 transitions.

under a wide array of experimental conditions. For example, in the normally-encountered high-spin electronic configurations ($O_h$ microsymmetry) of $Fe^{2+}(t_{2g}^4 e_g^2)$ and $Fe^{3+}(t_{2g}^3 e_g^2)$ it is always observed that the quadrupole splitting for compounds which contain the former ion is approximately 2-3 mm/s whereas the latter ion gives $\Delta$ near zero. A viable interpretation of this difference assumes that the additional $t_{2g}$ electron in $Fe^{2+}$ adds a very substantial non-spherical contribution to the efg as compared to the spherical

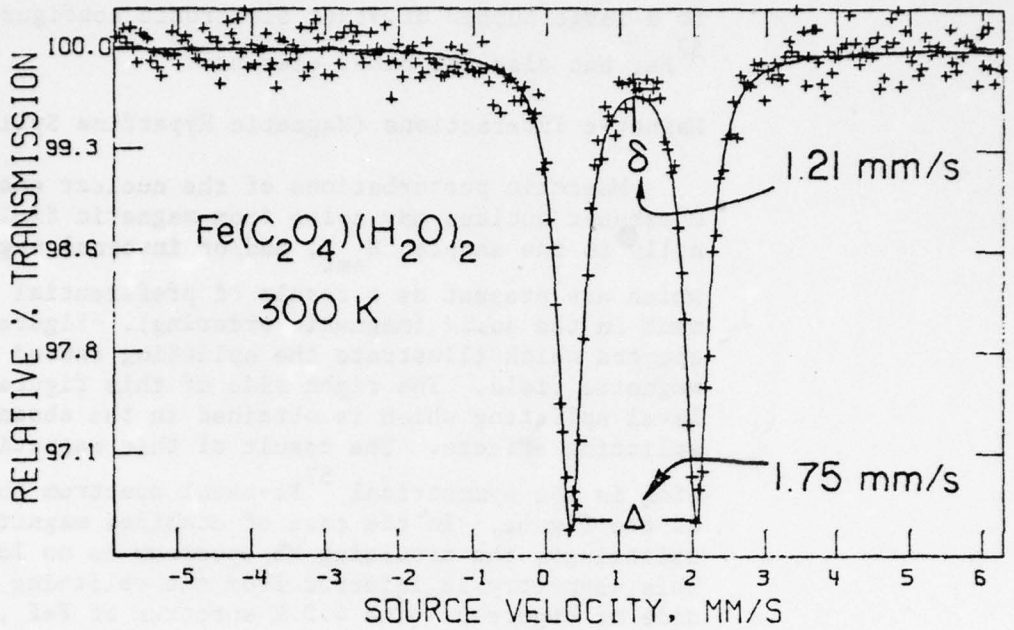


(a)

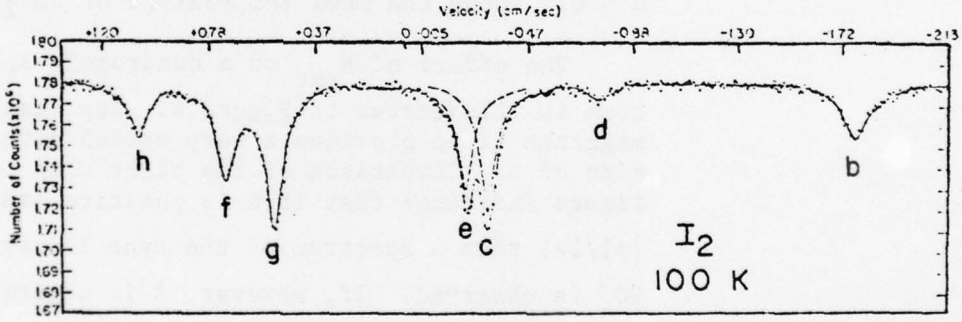


(b)

Figure 4. Quadrupole-split ME spectra for (a) $Fe(C_2O_4)(H_2O)_2$ relative to Fe metal [taken from Wrobleski, J. T., and Brown, D. B., 1979, Inorg. Chem., 18,] and (b) $I_2$ relative to $^{66}Zn^{129}Te$ source [taken from Pasternak, M., Simopoulos, A., and Hazony, Y., 1965, Phys. Rev., 140, p. A1892].

(half-filled) ferric configuration. By contrast, low-spin ferrous complexes ($t_{2g}^6 e_g^0$) have $\Delta \sim 0.0$ mm/s, whereas low-spin ferric complexes ($t_{2g}^5 e_g^0$) have $\Delta \sim 0.5$ mm/s. These arguments may be extended

to a large number of other electronic configurations, not only for $^{57}Fe$, but also for other elements.

Magnetic Interactions (Magnetic Hyperfine Splitting)

Magnetic perturbations of the nuclear energy levels in a Mössbauer nucleus may arise from magnetic fields applied externally to the sample, $H_{ext}$, and/or internal magnetic fields, $H_{int}$, which are present as a result of preferential electron spin alignment in the solid (magnetic ordering). Figure 5 depicts two spectra which illustrate the splitting caused by an internal magnetic field. The right side of this figure shows the spin level splitting which is obtained in the absence of quadrupole splitting effects. The result of this magnetic hyperfine splitting is the symmetrical $^{57}Fe$-metal spectrum shown at the bottom of the figure. In the case of combined magnetic and quadrupole splittings, the resulting ME spectrum is no longer symmetrical. This asymmetry is inferred from the splitting diagram on the left side of Figure 5. The 4.2 K spectrum of $FeF_2$, illustrated at the top of the figure, shows the effect of combined magnetic and quadrupole hyperfine perturbations on the nuclear spin levels. It should be noted that above the Curie temperature of iron metal its ME spectrum consists of a single absorption which indicates $\Delta \sim 0$. Above the Neél temperature of $FeF_2$ $\Delta \sim +2.8$ mm/s.

The effect of $H_{ext}$ on a quadrupole split $1/2 \leftrightarrow 3/2$ ME spectrum is illustrated in Figure 6. Application of a large external magnetic field provides a very useful method for determining the sign of $\Delta$. Comparison of the right with the left side of the figure indicates that if $\Delta$ is positive (that is $|\pm 3/2\rangle$ lie above $|\pm 1/2\rangle$) then a spectrum of the type illustrated for $[Fe^{II}(H_2O)_6]SO_4$ is observed. If, however, $\Delta$ is negative then an essentially mirror image ME spectrum results, as illustrated for $[Fe^{II}(H_2O)_6]SiF_6$. One must remember that if $\eta \neq 0$ the magnetically-perturbed spectra are more complicated. The effect of $\eta > 0$ on these spectra is discussed in several of the general references.

APPLICATION OF ME SPECTROSCOPY TO MIXED-VALENCE COMPOUNDS

The type of ME spectra observed for mixed-valence compounds depends on the relative rate of Mössbauer nuclear excited state decay $\underline{k}_n$ compared to the rate of intervalence electron transfer $\underline{k}_e$. Three spectral regimes are experimentally encountered. In

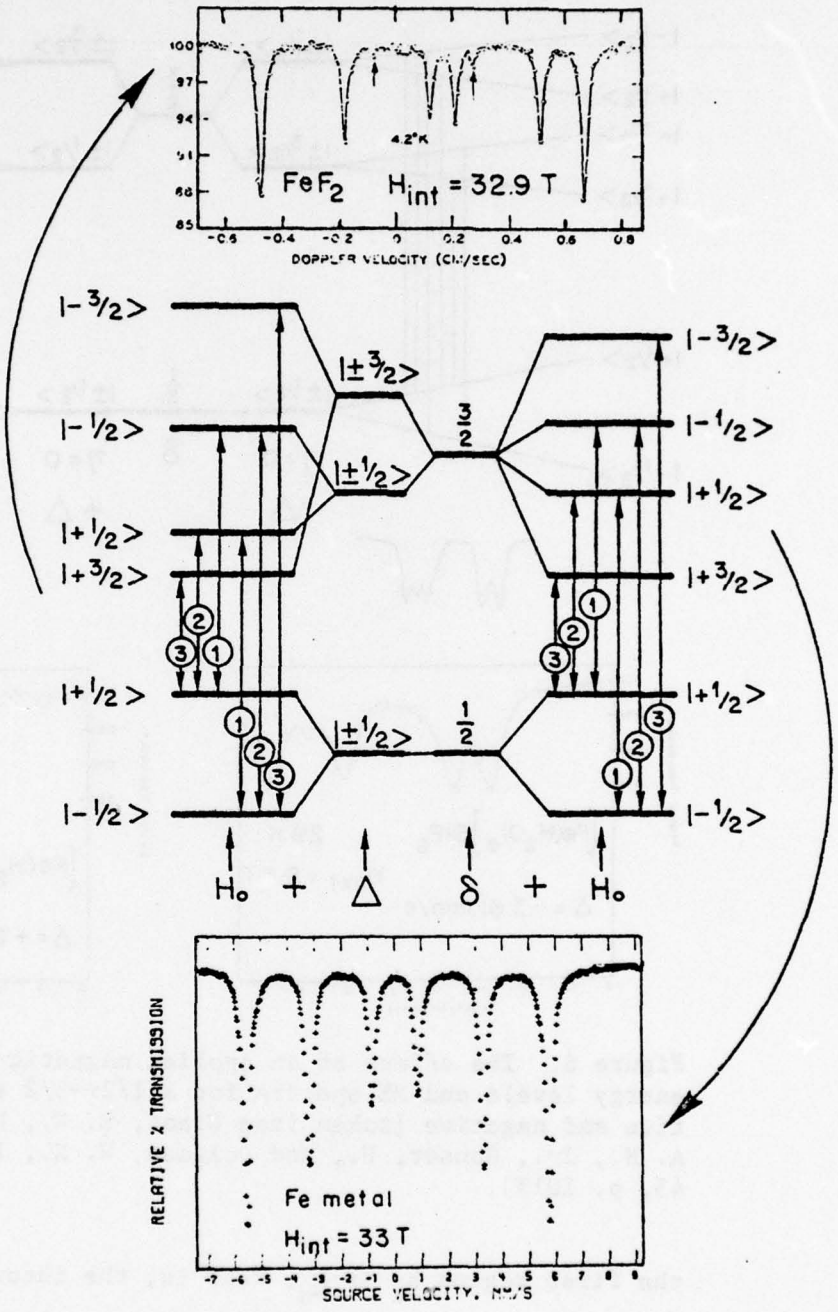


Figure 5. The effect of magnetic and magnetic + quadrupole hyperfine splitting on the 1/2 and 3/2 nuclear spin levels. The arrows on the spectrum of $FeF_2$ refer to two weak absorptions which arise from $|-1/2\rangle \leftrightarrow |+3/2\rangle$ and $|+1/2\rangle \leftrightarrow |-3/2\rangle$ transitions which are formally forbidden by the M1 selection rules [taken from Wertheim, G. K., and Buchanan, D. N. E., 1967, Phys. Rev., 161, p. 478].

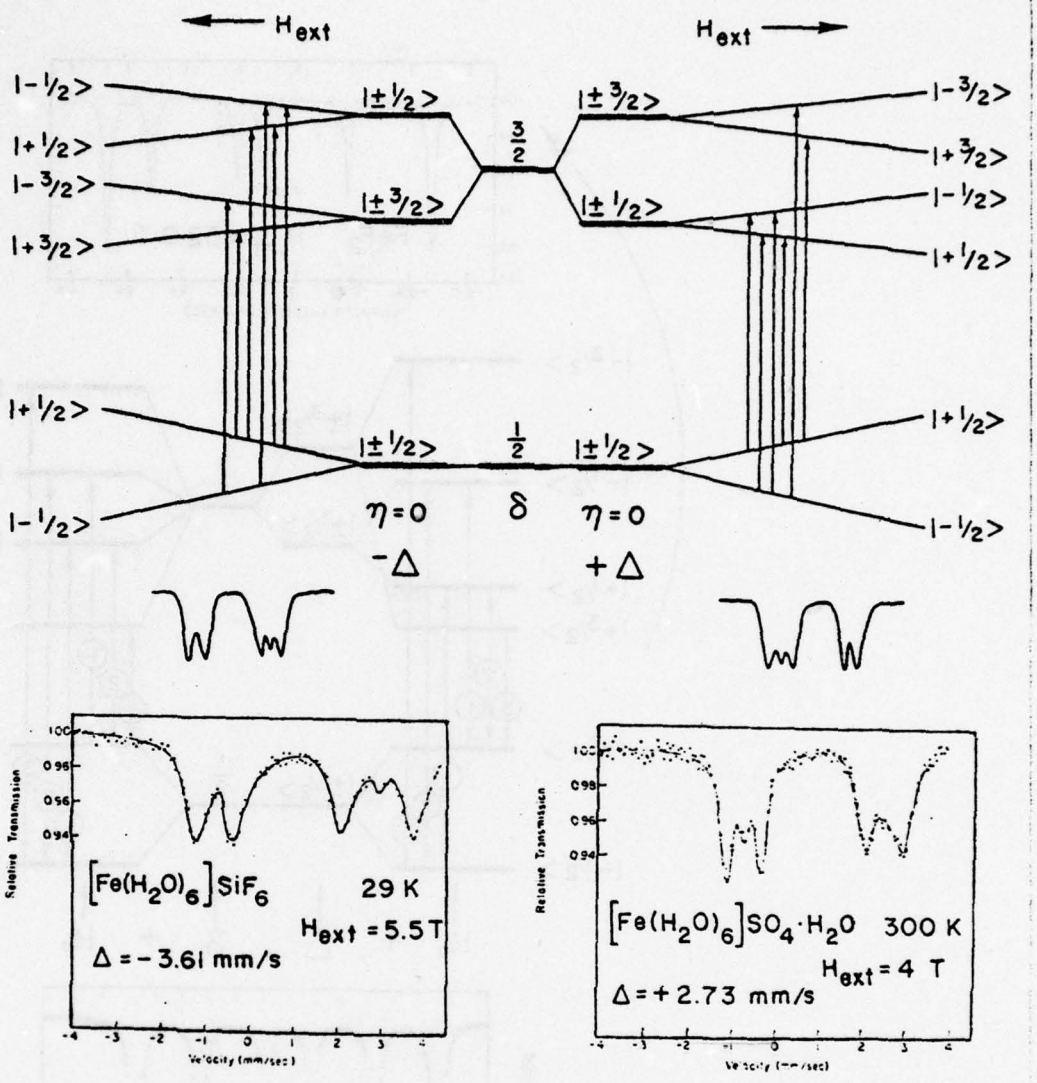


Figure 6. The effect of an applied magnetic field on the nuclear energy levels and ME spectra for a 1/2↔3/2 system with Δ positive and negative [taken from Grant, R. W., Wiedersich, H., Muir, A. N., Jr., Gonser, U., and Delgass, W. N., 1966, J. Chem. Phys., 45, p. 1015].

the first regime $\underline{k}_e << \underline{k}_n$, that is, the intervalence electron transfer rate is much slower than the nuclear excited state relaxation rate. Under this condition, discrete (deeply-trapped) oxidation states are observed on the ME time scale. In the second regime $\underline{k}_e >> \underline{k}_n$, which implies that the rate of intervalence electron transfer greatly exceeds the nuclear excited state decay rate. If this criterion is met, the ME records a spectrum which is the

weighted <u>average</u> of the individual oxidation state spectra. In the third regime $\underline{k}_e \cong \underline{k}_n$ and ME spectra are observed which are <u>intermediate</u> between those of the first and second regimes. In the third regime ME spectra are very temperature sensitive in response to the exponential temperature dependence of $\underline{k}_e$.

It is obvious that information about the dynamic aspects of mixed valency is accessible from ME experiments provided a suitable range of temperature (or perhaps pressure) is found such that $\underline{k}_e \cong \underline{k}_n$. Unfortunately many mixed-valence materials cannot withstand these experimental conditions or else the recoilless fraction of the particular nuclide under investigation is so small as to render the ME ineffective. Because of these factors only a relatively few mixed-valence compounds have provided the type of information about electron transfer rates in solids which is theoretically possible with the ME. Several of these systems, and compounds which show limiting behavior, are discussed in the following sections.

Compounds with $\underline{k}_e << \underline{k}_n$

Although compounds with $\underline{k}_e << \underline{k}_n$ fail to show mixed-valence interactions on the Mössbauer time scale, the ME does provide useful information about their structural and electronic properties. ME spectra of these materials are normally analyzed in terms of a simple superposition of the ME spectra of the individual oxidation site fragments. An example of this analysis is illustrated in Figure 7. Here the ME spectrum of mixed-valence $Fe_2F_5 \cdot 7H_2O$ (d) is compared with spectra of $[Fe(II)(H_2O)_6]SO_4 \cdot H_2O$ (a), $K_2[Fe(III)F_5(H_2O)]$ (b), and a 1:1 mixture of $[Fe(II)(H_2O)_6]SO_4 \cdot H_2O$ and $K_2[Fe(III)F_5(H_2O)]$ (c). The similarity of (c) and (d) strongly suggests that $Fe_2F_5 \cdot 7H_2O$ be formulated as $[Fe(II)(H_2O)_6][Fe(III)F_5(H_2O)]$ (1).

In the spectrum of $Fe_2F_5 \cdot 7H_2O$ (Figure 7d) the area ratio of the Fe(III) to the Fe(II) quadrupole doublet, $\underline{A}(Fe^{3+})/\underline{A}(Fe^{2+})$, is 1.0. This ratio is consistent with the ratio of ferric to ferrous ion determined by chemical analysis. Because the recoilless fraction may vary from site to site in a mixed-valence material, the areas of various ME absorptions in these compounds are not necessarily a direct measure of the relative amounts of the different oxidation states. Nonetheless, as in $Fe_2F_5 \cdot 7H_2O$, it is frequently observed that sites with different oxidation states in similar chemical environments do have comparable recoilless fractions, and therefore site populations may be at least semi-quantitatively related to ME area ratios.

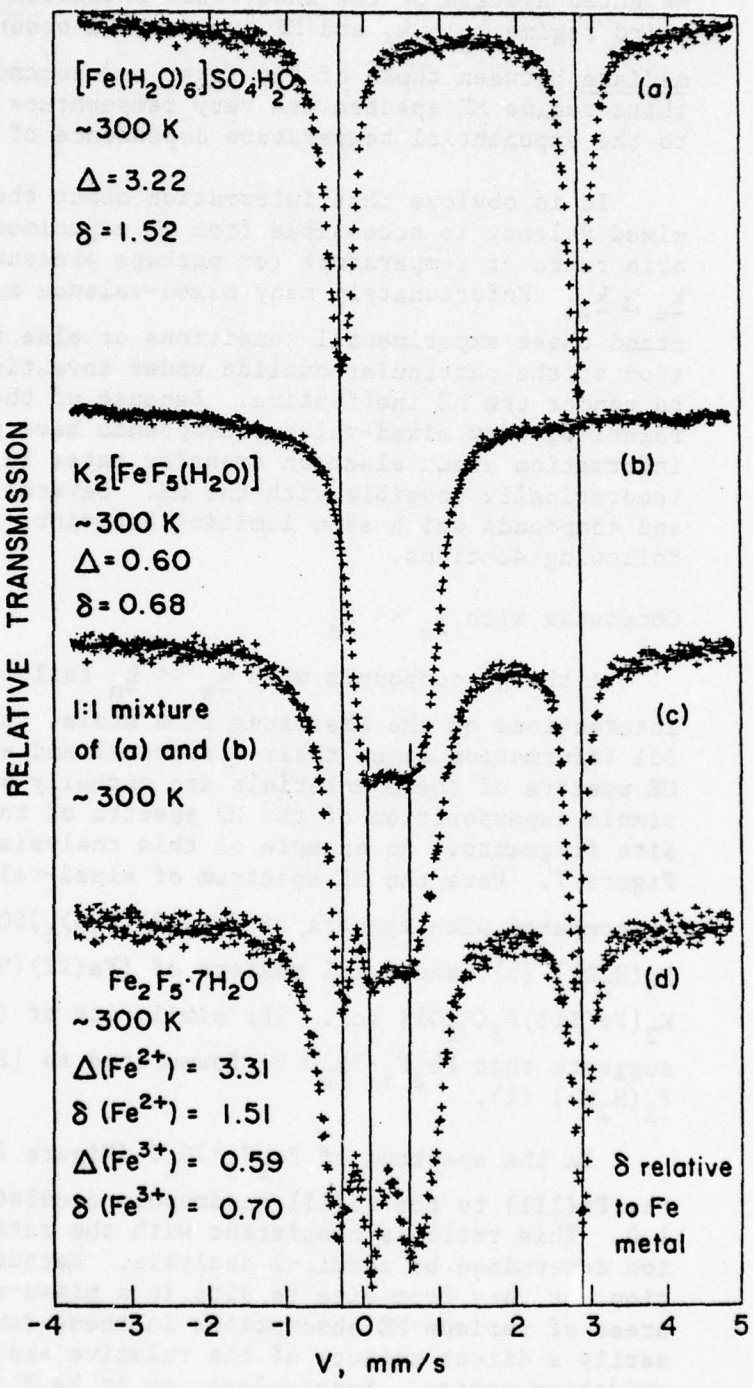


Figure 7. Room temperature $^{57}$Fe Mössbauer spectra of (a) $[Fe(H_2O)_6]SO_4 \cdot H_2O$, (b) $K_2[FeF_5(H_2O)]$, (c) 1:1 mixture of (a) and (b), and (d) $Fe_2F_5 \cdot 7H_2O$.

A somewhat similar analysis has been extremely useful in clarifying the nature of the Prussian Blues (2,3). By using the ME, it has been possible to show that Prussian Blue and Turnbull's Blue (prepared by eqs. 5 and 6, respectively) are in fact identical, and that both contain low-spin Fe(II) ($C_6$ coordination) and

$$Fe_2(SO_4)_3 + K_4Fe(CN)_6 \rightarrow Fe(III)_4[Fe(II)(CN)_6]_3 \qquad (5)$$

$$FeCl_2 + K_3Fe(CN)_6 \rightarrow Fe(III)_4[Fe(II)(CN)_6]_3 \qquad (6)$$

high spin Fe(III) ($N_6$ or $N_4O_2$ coordination). The ME spectral overlap due to the presence of both types of iron site makes interpretation difficult, but the problem is simplified by selective isotopic substitution. Naturally-occurring iron contains only 2.17% $^{57}Fe$, the ME active nuclide. By labelling one of the reactants in eqs. 5 or 6 with either $^{57}Fe$ or $^{56}Fe$, materials can be prepared whose ME spectra show either selective enhancement or disappearance of absorption due to a particular site. This substitution allows not only identification of spectral components, but in the case of eq. 6 demonstrates that the product forms as the result of electron transfer, rather than ligand transfer. Of course, the use of isotopic substitution in this fashion is dependent on the iron sites maintaining their uniqueness throughout the reaction.

Several Ru-containing mixed-valence compounds have been studied with $^{99}Ru$ ME spectroscopy. Because of the low recoilless fraction of $^{99}Ru$ ($\gamma_M$ = 89.36 keV) above 4.2 K, ME spectra are difficult to obtain at temperatures where thermally-activated electron-transfer processes are likely to occur. Rather, low-temperature ME spectra have been used to discriminate between the limiting cases of Robin and Day Class II and Class III behavior (4) (or of trapped versus delocalized electrons). ME spectra of representative Ru mixed-valence compounds are illustrated in Figure 8. From the earlier discussion (see Figure 3) the $^{99}Ru$ ME spectrum of a single type of Ru is expected to consist of five absorptions because $^{99}Ru$ has ground- and excited-state nuclear spins of 5/2 and 3/2, respectively. In fact, two line quadrupole split spectra are normally observed for $^{99}Ru$ compounds. This two line splitting pattern arises because the nuclear quadrupole moment ratio $Q(3/2)/Q(5/2)$ is very large for $^{99}Ru$. Therefore only transitions from the nearly degenerate $m_I$ = ±5/2, ±3/2, and ±1/2 components of the $I$ = 5/2 ground state to the strongly quadrupole-split $m_I$ = ±3/2 and ±1/2 components of the $I$ = 3/2 excited state are observed.

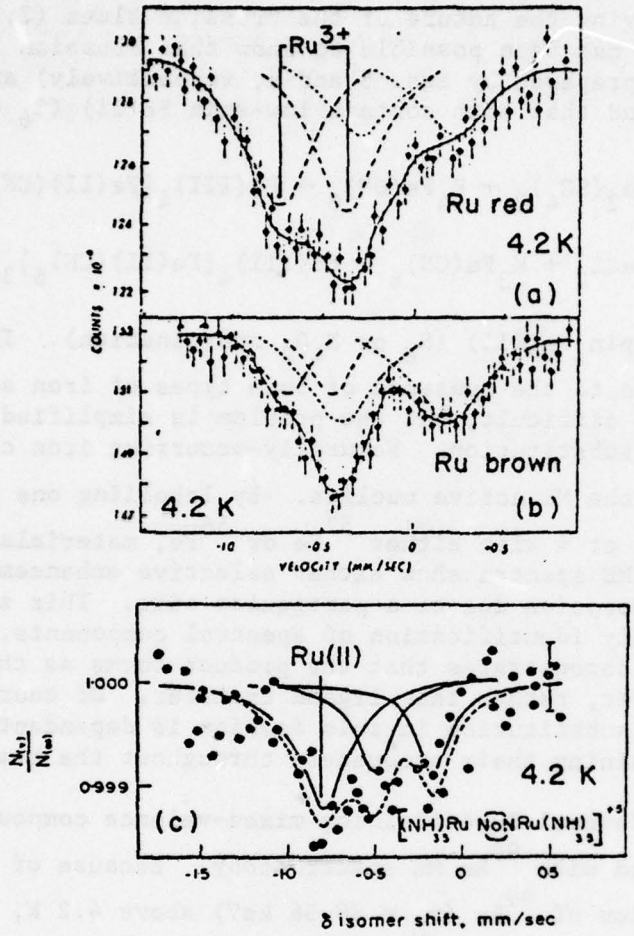


| Ru(III) | Ru(IV) |
|---|---|
| δ = −0.55 | δ = −0.06 |
| Δ = 0.36 | Δ = 0.53 |

| Ru(III) | Ru(IV) |
|---|---|
| δ = −0.52 | δ = −0.10 |
| Δ = 0.25 | Δ = 0.59 |

| Ru(II) | Ru(III) |
|---|---|
| δ = −0.79 | δ = −0.32 |
| Δ ~ 0 | Δ = 0.34 |

Figure 8. 4.2 K $^{99}$Ru Mössbauer spectra of (a) Ruthenium Red, (b) Ruthenium Brown, and (c) Creutz and Taube ion, all of which are trapped-valence, Class II compounds.

Isomer shifts for the three illustrated oxidation states increase in the order Ru(IV) > Ru(III) > Ru(II) as anticipated on the basis of increased s-electron shielding by valence d electrons in this series (Table I). In the case of Ruthenium Red, $[(NH_3)_5Ru(III)ORu(IV)(NH_3)_4ORu(III)(NH_3)_5]^{6+}$ [Figure 8, spectrum (a)], and its one-electron oxidation product Ruthenium Brown, $[(NH_3)_5Ru(IV)ORu(III)(NH_3)_4ORu(IV)(NH_3)_5]^{7+}$ [spectrum (b)], the Ru(III)/Ru(IV) area ratios are 2/1 and 1/2, respectively (5). Figure 8 (c) shows the $^{99}$Ru ME spectrum of the Creutz and Taube ion (6),

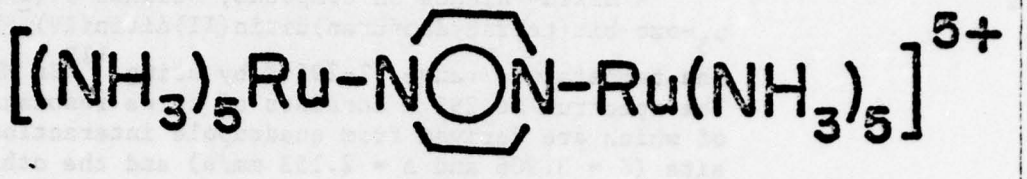

This spectrum is clearly consistent with the presence of trapped Ru(II) and Ru(III) valences.

This example points out the clear utility of ME spectroscopy as a probe for the extent of electron delocalization. For a totally-delocalized (Class III) material, all valence sites must be equivalent under any conditions of measurement. By contrast, valence sites which are trapped (Class II) but which may be interchanged by electron transfer may appear to be equivalent or inequivalent depending upon the relative rates of the electron transfer and the measuring technique. The literature contains a number of conflicting claims concerning the Creutz and Taube ion, but the ME evidence is unambiguous in demonstrating that this ion is a Class II material. Because of the exponential temperature dependence of the (phonon-assisted) electron-transfer process, at temperatures much greater than 4.2 K even very fast measurement techniques may fail to detect trapped valence states.

Several other compounds in which $k_e << k_n$ have been investigated by ME spectroscopy. Among these are materials of the type $A_2SbX_6$ in which A is a monovalent cation and X is a halide. These compounds were previously thought to be rare examples of Sb(IV) compounds. Original examination of $^{121}$Sb ME spectrum of $Cs_2SbCl_6$ indicated that discrete Sb(III) ($\delta$ = -19.0 mm/s rel. to $Ba^{121}SnO_3$) and Sb(V) ($\delta$ = -3.0 mm/s) sites were present at 4.2 K. At higher temperatures additional absorptions with intermediate $\delta$ values were observed (7). These additional absorptions have not been found in more recent work (8), and on the basis of ME and infrared results these compounds are presently thought to have the composition $A_4\{[Sb(III)X_6][Sb(V)X_6]\}$.

A mixed-valence linear chain polymer, $Fe(II,III)(C_2O_4)(H_2O)_{1.4}Br_{0.6}$, has recently been studied by zero-field $^{57}$Fe ME spectroscopy (9). In the temperature range 30-400 K the spectrum consists of superimposed Fe(II) and Fe(III) quadrupole doublets. At 30 K the resonant absorptions begin to broaden and below ca. 25 K a large number of lines appear in the spectrum. This complicated low-temperature spectrum results from the superposition of magnetic hyperfine absorptions for the Fe(II) and Fe(III) sites in this magnetically-ordered material.

A mixed-valence Sn compound, octakis-μ-(o-nitrobenzoato)-di-$\mu_3$-oxo-bis(tetrahydrofuran)ditin(II)ditin(IV), has been studied in the temperature range 77-295 K by using $^{119}$Sn ME spectroscopy (10). The spectrum at 295 K consists of three resonant absorptions, two of which are derived from quadrupole interaction with the Sn(II) site ($\delta$ = 3.906 and $\Delta$ = 2.133 mm/s) and the other from the Sn(IV) site ($\delta$ = -0.021 mm/s).

Temperature-dependent ME spectra of mixed-valence meso-tetraferrocenylporphyrin, whose structure is shown in Figure 9(a), have recently been investigated (11). Spectra taken at 295, 90, and 4.2 K are illustrated in Figure 9(b). Although these spectra are not characteristic of oxidation state averaging, there is a very strong temperature dependence to the Fe(II)/Fe(III) line intensity

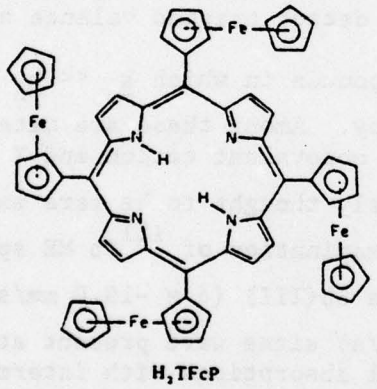


(a)

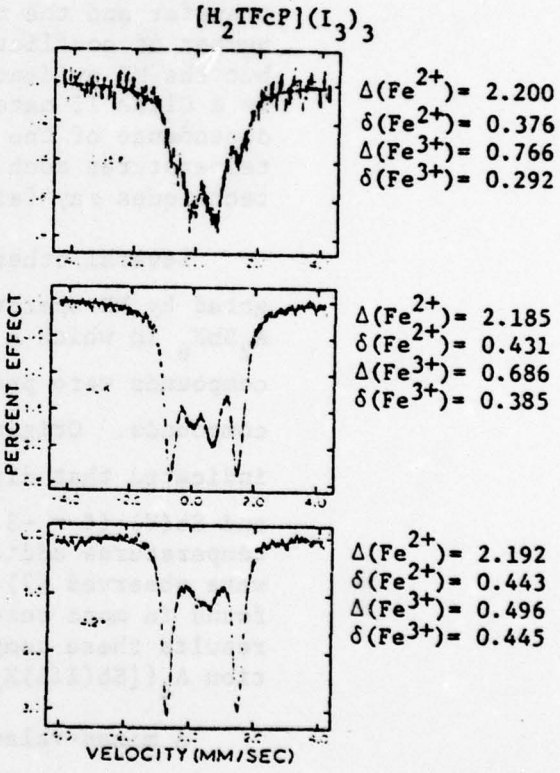


(b)

Figure 9. (a) Structure of Fe(III)$_3$Fe(II)-tetraferrocenylporphyrin. (b) $^{57}$Fe ME spectra of this cation at 295, 90, and 4.2 K.

ratio. The authors (11) attribute this temperature dependence to a temperature-dependent intramolecular redox process in which electrons are transferred from ferricenium-like groups to the porphyrin ring. An alternative explanation for these observations was discussed by the authors, but ultimately rejected by them. As discussed above, the areas of ME absorptions are not necessarily a direct reflection of individual valence populations. Because the recoilless fraction may have a different temperature dependence for each valence site in a mixed-valence material, the area variations of these spectra may simply reflect such differences.

Many naturally-occurring substances, including a large number of minerals, are mixed-valence iron compounds in which intervalence electron exchange is slow. Because of the wide distribution of these materials, the ME has become a powerful tool in geology, the analysis of art objects, and archaeology. As only one of many examples, the ME has been used to study two different forms of pottery shards, one red and the other gray (12). Both of these types of shards were found in Iran and dated at approximately 3000 B.C. ME spectra of these shards were compared with ME spectra of local clays fired at various temperatures and the relative amounts of $Fe^{3+}$ and $Fe^{2+}$ in the samples were determined. These investigations led to the conclusion that the red and gray pottery shards both had a local origin but differed in their firing temperature and in the use of oxidizing or reducing atmospheres in the firing process.

Compounds with $k_e >> k_n$

Mixed-valence materials in which the electron transfer rate is much larger than the Mössbauer nuclear excited state relaxation rate are expected to possess intermediate ME isomer shifts and quadrupole splittings which are weighted averages of $\delta$ for the isolated oxidation states. (This averaging process is only an approximation, however, because of the undetermined effect of covalency on the isomer shift of the mixed-valence state. Thus one would anticipate that the degree of covalency in the mixed-valence state might be different than the degree of covalency in the isolated oxidation states.) The observation in the ME spectrum of a single type of absorption for a material which is formally mixed valent cannot by itself establish the material as belonging to Class III although it can set a lower limit on the rate of an electron transfer process. As discussed in the following section, Class II materials in which electron exchange is rapid on the Mössbauer time scale exhibit averaged spectra of this type, but at some temperature the distinct oxidation states become indistinguishable. If the barrier to electron transfer is zero ($k_e = \infty$, Robin and Day Class III behavior) then there is no temperature at which oxidation state ordering is observed. Although there are very few

examples of Class III mixed-valence compounds which contain Mössbauer-active nuclei, this situation apparently obtains for the mixed-valence material $SmB_6$ in which the $^{149}Sm$ isomer shift (-0.38 mm/s at 1 K) is the weighted average of the isomer shift of $Sm^{2+}$ and $Sm^{3+}$ compounds [-0.92 ($SmF_2$) and -0.1 ($SmF_3$) mm/s, respectively] (13).

Another example of a material in which $\underline{k}_e >> \underline{k}_n$ is the cubic phase of $Fe_3O_4$. This inverse spinel Fe(II,III) oxide phase which exists above 120 K gives rise to a twelve line magnetically-ordered ME spectrum (14). One six line hyperfine pattern arises from trapped $Fe^{3+}$ ions in the tetrahedral sites while the other six line pattern is due to oxidation state averaged iron ions in octahedral sites. Because $Fe_3O_4$ undergoes a structural phase transition at 120 K it is not possible to determine if the Class III behavior of the cubic phase persists to very low temperatures.

Perhaps the most striking examples of non-integral oxidation state materials, and certainly the most extensively studied, are compounds related to biferrocene, I. Although isomer shifts for

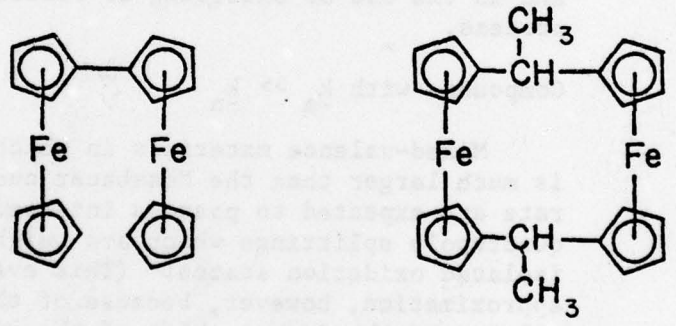


species similar to ferrocene and ferricenium ion are virtually identical, the large difference in quadrupole splittings (ferrocene $\Delta$ = 2.4 mm/s and ferricenium ion $\Delta \simeq$ 0-0.8 mm/s) permits facile identification of $Fe^{2+}$ and $Fe^{3+}$ sites in similar compounds. Thus, monooxidized salts of I are shown by ME spectroscopy to contain trapped valence states with $\Delta(Fe^{2+})$ = 2.14 mm/s and $\Delta(Fe^{3+})$ = 0.288 mm/s (15). Trapped valences are also observed for [1.1] ferrocenophanes such as II (16). However, the monooxidized salts of both biferrocenylene, III, and [2.2]ferrocenophane-1,13-diyne, IV, exhibit intermediate (averaged) oxidation state ME spectra (16, 17). Thus, at 78 K salts of the monocations of III and IV give ME

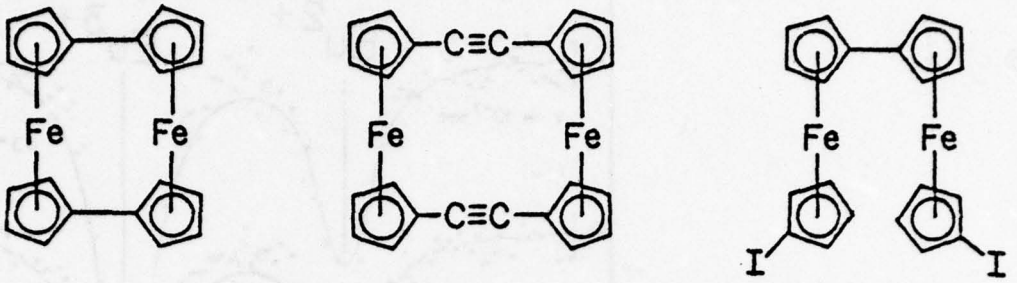


spectra which consist of single quadrupole doublets with $\Delta$ = 1.78 and 1.61 mm/s, respectively. These $\Delta$ values are approximately the averages of those obtained for the individual $Fe^{2+}$ and $Fe^{3+}$ complexes. This averaging of $\Delta$ values indicates equivalence of all Fe sites on the Mössbauer time scale. Because in each case the sites remain averaged at 4.2 K, the monocations of III and IV are clearly Class III compounds. Surprisingly, the monooxidized $I_3^-$ salt of 1',6'-diiodobiferrocene, V, which lacks the rigid, conjugated structural features of III and IV, also exhibits valence state delocalization. The coupling mechanisms by which ion sites in III-V are rendered equivalent are not at present understood.

Compounds with $\underline{k}_e \sim \underline{k}_n$

Compounds in which the rate of nuclear excited state decay and the rate of intervalence electron transfer are comparable are probably the most interesting cases for study by ME techniques. In principle it is possible to extract rates of electron transfer, and consequently energy barriers to electron transfer, from a study of the temperature dependence of ME spectra of these materials. In these cases the ME spectra vary in a predictable fashion with the rate of electronic relaxation because $\underline{k}_n$ is essentially independent of chemical environment and temperature.

Possibly the most thoroughly understood mixed-valence material in which $\underline{k}_e \sim \underline{k}_n$ is $Eu_3S_4$, $Eu(III)_2Eu(II)S_4$. In this compound all Eu ions occupy crystallographically-equivalent sites at room temperature. Temperature-dependent $^{151}Eu$($\tau_n$ = 8.8 ns) ME spectra of $Eu_3S_4$ are illustrated in Figure 10 (18). At 85 K the spectrum consists of two absorptions for which $\delta \simeq$ -12.0 mm/s ($Eu^{2+}$ site) and $\delta \simeq$ 0.0 mm/s ($Eu^{3+}$ site) in the approximate ratio 1:2, respectively. The spectrum of $Eu_3S_4$ at 4.2 K (19) is essentially unchanged. (No quadrupole splitting of either site is observed because the quadrupole interaction is considerably less than the

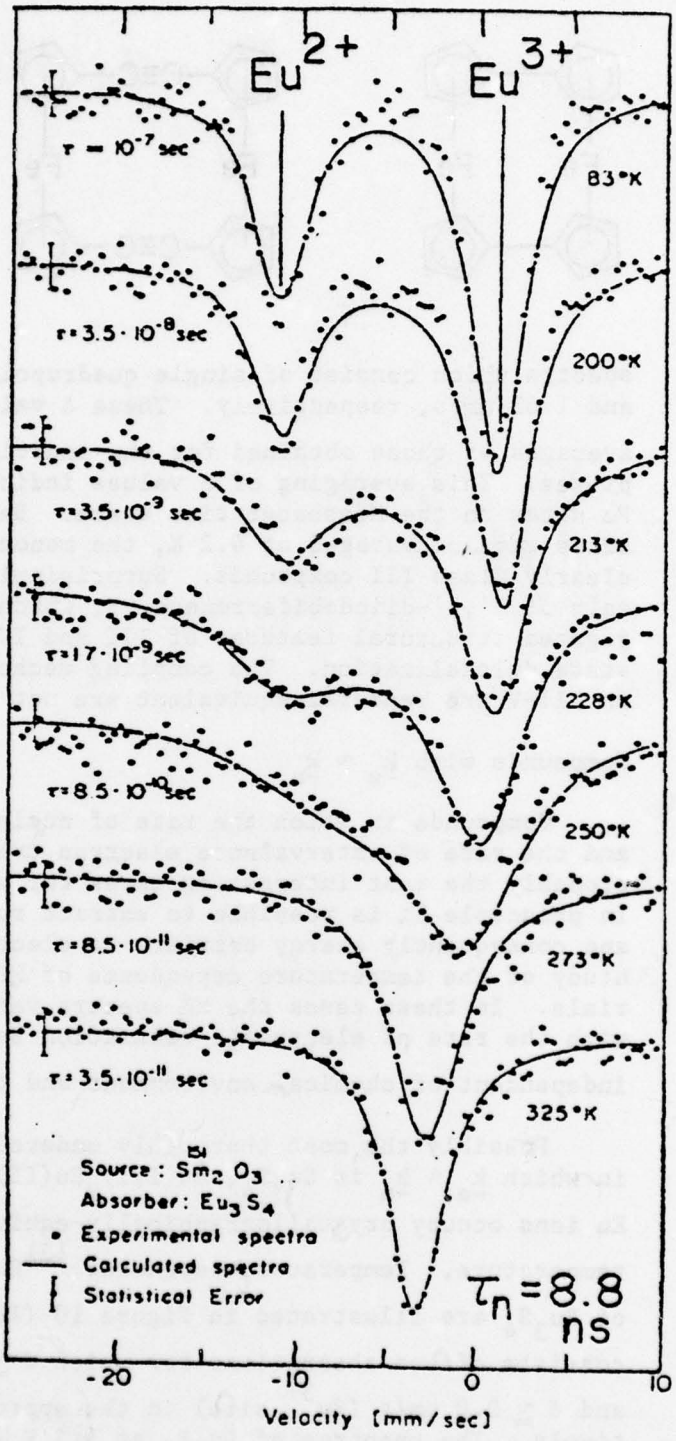


Figure 10. Temperature variation of the $^{151}Eu$ ME spectrum of $Eu_3S_4$ and fits for the relaxation model.

width of $\gamma_M$.) As the temperature is increased the resonant absorptions broaden and approach one another. At 325 K the spectrum consists of an unbroadened resonant absorption at $\delta \simeq -4$ mm/s. This high-temperature spectrum arises from the oxidation state averaged Eu sites. The high temperature isomer shift is exactly equal to the weighted average (eq. 7) of the $Eu^{2+}$ and $Eu^{3+}$ isomer shifts.

$$\delta_{average} = [2\delta(Eu^{3+}) + \delta(Eu^{2+})]/3 \qquad (7)$$

In order to determine the thermal barrier to electron transfer in $Eu_3S_4$ from ME data, the electron relaxation time, $\tau_e (\equiv 1/k_e)$, was obtained by fitting experimental spectra to the semi-quantum mechanical rate equations of Wickman (20). Resulting relaxation times are given in Figure 10. The electron relaxation times may be fit to an Arrhenius equation (eq. 8) where $E$ is the intervalence

$$\tau_e(T) = \tau_o \exp(E/k_B T) \qquad (8)$$

electron transfer energy barrier and $k_B$ is Boltzmann's constant. A plot of log $\tau_e$ versus $1/T$ for $Eu_3S_4$ gives $E = 0.24 \pm 0.03$ eV and $\tau_o = 25 \times 10^{-14}$ s. This value of $E$ is identical to the band gap energy for $Eu_3S_4$ determined by conductivity measurements. This congruence of experimental results demonstrates that the electronic relaxation phenomenon observed with ME spectroscopy is a consequence of an intervalence electron transfer process.

Electron hopping in the mixed-valence compound $[Fe(II)Fe(III)_2O(CH_3COO)_6(H_2O)_3]$ has recently been investigated by ME spectroscopy (21). The structure of this compound is shown below and several representative ME spectra in the range 17-300 K are illustrated in Figure 11. At 17 K the spectrum consists of quadrupole

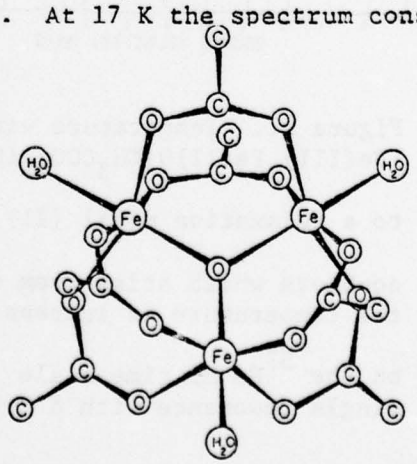

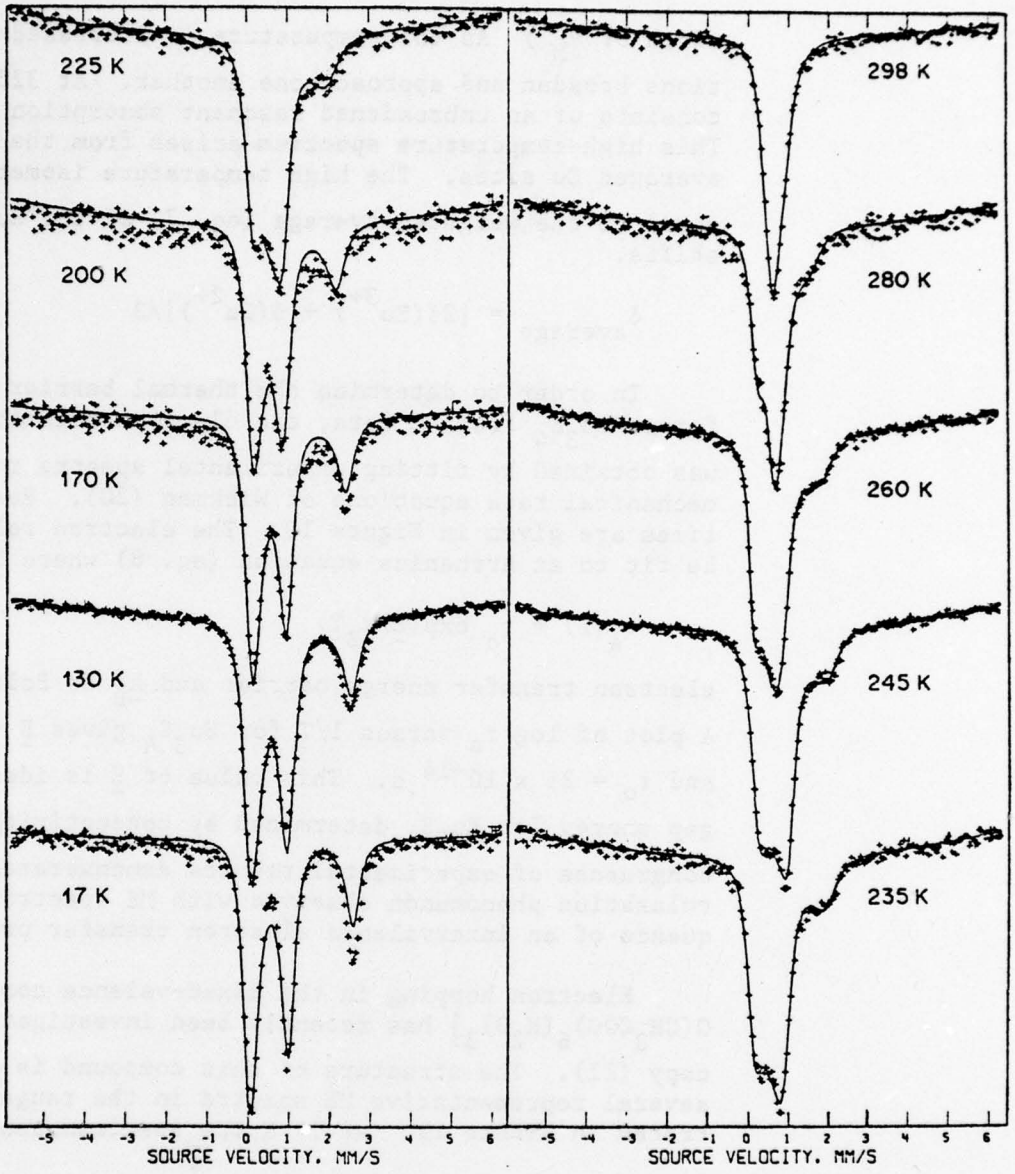


Figure 11. Temperature variation of the $^{57}$Fe ME spectrum of $[Fe(III)_2Fe(II)O(CH_3COO)_6(H_2O)_3]$. The solid lines represent fits to a relaxation model (21).

doublets which arise from discrete Fe(II) and Fe(III) sites. As the temperature is increased the sites become indistinguishable on the $^{57}$Fe ME time scale ($\tau_n$ = 98 ns) until finally at 295 K a single resonance with $\delta$ = 0.75 mm/s is obtained. It is interesting

to note that the quadrupole splitting "averages" to zero in the delocalized spectrum of this complex. This observation is consistent with a negative $\Delta Fe(II)/\Delta Fe(III)$ ratio (21). If a modified relaxation model based on the equations of Wickman (20) is applied to these data (21), the calculated spectra shown in Figure 11 are obtained. Relaxation times range from >2400 ns at 17 K to 65 ns at 225 K to 5 ns at 298 K. A plot of log $\tau_e$ vs. $1/\underline{T}$ yields an electron hopping barrier of 470 $cm^{-1}$. This value of $\underline{E}$ is consistent with a phonon-assisted electron transfer process in that infrared spectral studies (21) indicate that the asymmetric $Fe_3O$ stretching frequency of this compound is near 520 $cm^{-1}$. Although the symmetric $Fe_3O$ stretching absorption has not been observed, it is predicted to lie in the infrared at a frequency near $\underline{E}$ determined from ME studies. It is most likely this low-frequency $Fe_3O$ stretching mode which is responsible for intervalence electron transfer in this trimer.

In order to properly interpret electron hopping rates determined from ME measurements it is necessary to know the crystallographic distribution of oxidation sites. Thus in both $Eu_3S_4$ and $[Fe_3O(CH_3COO)_6(H_2O)_3]$ all the metal sites are equivalent both on the ME and X-ray crystallography time scales. In some instances not all of the metal centers are oxidation-state averaged on the ME time scale. The problem of deciding among which crystallographic sites electron hopping is occurring is particularly severe in the case of mixed-valence minerals as was recently shown for hematite-ilmenite (22). In the case of the silicate mineral ilvaite, $CaFe_2^{2+}Fe^{3+}Si_2O_8(OH)$, it is apparently necessary to include five quadrupole doublets in an analysis of the temperature dependent ME spectra of this material (23). In addition, the details of these spectra depend to a large extent on the geological history of the mineral specimens. Several other mixed-valence, iron-containing minerals, which have not been investigated in detail, appear to undergo thermal intervalence electron hopping with rates on the order of the ME time scale. These minerals include pentlandite $[(Ni,Fe)_9S_8]$ (24) and wustite ($Fe_{\sim 0.9}O$) (25).

Although the ME has the potential for probing directly the dynamics of intervalence electron transfer processes in materials with $\underline{k}_e \sim \underline{k}_n$, practical considerations limit its use. In particular, the ability to perform ME measurements over a wide temperature range, and hence a range of electron transfer rates, is limited to a few nuclei including iron and europium. Thus ruthenium complexes, such as the Creutz and Taube ion, can be examined by ME only near 4 K, and therefore the rapid intervalence electron

transfer which is known to occur at higher temepratures cannot be observed in ME experiments. Because of the exponential temperature dependence of the electron transfer process, many iron compounds might be expected to fulfill the condition $k_e \sim k_n$ at elevated temperatures. Although $^{57}Fe$ ME spectra can be obtained at elevated temperatures (>300 K), the thermal stability of the materials often is the limiting factor under these conditions.

## CONCLUSIONS

ME spectroscopy has proven to be an extremely useful tool for the study of both static and dynamic features of the mixed-valence state. Although a wide range of mixed-valence materials have been studied by ME spectroscopy, a large number of interesting systems remain uninvestigated. In addition, a good deal of fundamental theoretical work is required to fully understand the effects on ME spectra of electron transfer in mixed-valence solids. The unique ability of the ME to directly probe oxidation states insure its continuing use in the study of mixed-valence materials.

## ACKNOWLEDGEMENT

Our work in the area of mixed-valence chemistry has been supported in part by the Office of Naval Research.

## GENERAL REFERENCES ON THE MÖSSBAUER EFFECT

A. N. N. Greenwood and T. C. Gibb, "Mössbauer Spectrocopy," Chapman and Hall, London (1971).

B. T. C. Gibb, "Principles of Mössbauer Spectroscopy," Chapman and Hall, London (1976).

C. V. I. Goldanskii and E. F. Makarov, "Fundamentals of Gamma-Resonance Spectroscopy," Chapter 1 in "Chemical Applications of Mössbauer Spectroscopy," V. I. Goldanskii and R. H. Herber, Eds.; Academic Press, New York (1968).

D. R. L. Cohen, "Elements of Mössbauer Spectroscopy," Chapter 1 in "Applications of Mössbauer Spectroscopy," Vol. 1, R. L. Cohen, Ed.; Academic Press, New York (1976).

E. G. M. Bancroft, "Mössbauer Spectroscopy An Introduction for Inorganic Chemists and Geochemists," John Wiley and Sons, New York (1973).

SPECIAL REFERENCES


1. Walton, E. G., Corvan, P. J., Brown, D. B., and Day, P.: 1976, Inorg. Chem. 15, p. 1737.

2. Maer, K., Jr., Beasley, M. L., Collins, R. L., and Milligan, W. O.: 1968, J. Am. Chem. Soc. 90, p. 3201.

3. Bonnette, A. K., Jr., and Allen, J. F.: 1971, Inorg. Chem. 10, p. 1613.

4. Robin, M. B., and Day, P.: 1967, Adv. Inorg. Chem. Radiochem. 10, p. 247.

5. Clausen, C. A., III, Prados, R. A., and Good, M. L.: 1971, Inorg. Nucl. Chem. Lett. 7, p. 485.

6. Creutz, C., Good, M. L., and Chandra, S.: 1973, Inorg. Nucl. Chem. Lett. 9, p. 171.

7. Aleksandrov, A. Y., Ionov, S. P., Baltrunas, D. A., and Makarov, E. F.: 1972, Soviet Phys. JETP Lett. 16, p. 147.

8. Longworth, G., and Day, P.: 1976, Inorg. Nucl. Chem. Lett. 12, p. 451.

9. Wrobleski, J. T., and Brown, D. B.: 1979, Inorg. Chem. 18, p. 0000.

10. Ewings, P. F. R., Harrison, P. G., Morris, A., and King, T. J.: 1976, J. Chem. Soc. Dalton Trans., p. 1602.

11. Wollmann, R. G., and Hendrickson, D. N.: 1977, Inorg. Chem. 16, p. 3079.

12. Bouchez, R., Coey, J. M. D., Coussement, R., Schmidt, K. P., Van Rossum, M., Aprahamian, J., and Deshayes, J.: 1974, Proc. Int. Conf. Appl. Mössbauer Effect, Bendor, 1974, J. Phys. Colloq. 35, C6, p. 541.

13. Varma, C. M.: 1978, Rev. Mod. Phys. 48, p. 219.

14. Banerjee, S. K., O'Reilly, W., and Johnson, C. E.: 1967, J. Appl. Phys. 38, p. 1289.

15. Cowan, D. O., LeVanda, C., Park, J., and Kaufman, F.: 1973, Acc. Chem. Res. 6, p. 1.

16. Morrison, W. H., Jr., and Hendrickson, D. N.: 1975, Inorg. Chem. 14, p. 2331.

17. Motoyama, I., Watanabe, M., and Sano, H.: 1978, Chem. Lett., p. 513.

18. Berkooz, O., Malamud, M., and Shtrikman, S.: 1968, Sol. State Comm. 6, p. 185.

19. Görlich, E., Hyrnkiewicz, H. U., Kmiec, R., Latka, K., and Tomola, K.: 1974, Phys. Stat. Sol. (b) 64, p. K147.

20. Wickman, H. H.: 1966, Mössbauer Effect Methodology 2, p. 39. Wickman, H. H., Klein, M. P., and Shirley, D. A.: 1966, Phys. Rev. 152, p. 345.

21. Dziobkowski, C. T., Wrobleski, J. T., and Brown, D. B.: Inorg. Chem., submitted for publication.

22. Warner, B. N., Shive, P. N., Allen, A. L., and Terry, C. J.: 1972, Geomag. Geoelectr. 24, p. 353.

23. Nolet, D. A.: 1978, Sol. State Comm. 28, p. 719. A three quadrupole doublet analysis of ilvaite has been presented: Heilmann, I. U., Olsen, N. B., and Olsen, J. S.: 1977, Phys. Scripta 15, p. 285.

24. Vaughan, D. J., and Ridout, M. S.: 1971, J. Inorg. Nucl. Chem. 33, p. 741.

25. Elias, D. J., and Linnett, J. W.: 1969, Trans. Farad. Soc. 65, p. 2673.

# TECHNICAL REPORT DISTRIBUTION LIST, 053

| | No. Copies |
|---|---|
| Dr. R. N. Grimes<br>University of Virginia<br>Department of Chemistry<br>Charlottsville, Virginia 22901 | 1 |
| Dr. M. Tsutsui<br>Texas A&M University<br>Department of Chemistry<br>College Station, Texas 77843 | 1 |
| Dr. M. F. Hawthorne<br>University of California<br>Department of Chemistry<br>Los Angeles, California 90024 | 1 |
| Dr. W. B. Fox<br>Naval Research Laboratory<br>Chemistry Division<br>Code 6130<br>Washington, D. C. 20375 | 1 |
| Dr. J. Adcock<br>University of Tennessee<br>Department of Chemistry<br>Knoxville, Tennessee 37916 | 1 |
| Dr. A. Cowley<br>University of Texas<br>Department of Chemistry<br>Austin, Texas 78712 | 1 |
| Dr. W. Hatfield<br>University of North Carolina<br>Department of Chemistry<br>Chapel Hill, North Carolina 27514 | 1 |
| Dr. D. Seyferth<br>Massachusetts Institute of Technology<br>Department of Chemistry<br>Cambridge, Massachusetts 02139 | 1 |
| Dr. M. H. Chisholm<br>Department of Chemistry<br>Indiana University<br>Bloomington, Indiana 47401 | 1 |
| Dr. B. Foxman<br>Brandeis University<br>Department of Chemistry<br>Waltham, Massachusetts 02154 | 1 |
| Dr. T. Marks<br>Northwestern University<br>Department of Chemistry<br>Evanston, Illinois 60201 | 1 |
| Dr. G. Geoffrey<br>Pennsylvania State University<br>Department of Chemistry<br>University Park, Pennsylvania 16802 | 1 |
| Dr. J. Zuckerman<br>University of Oklahoma<br>Department of Chemistry<br>Norman, Oklahoma 73019 | 1 |
| Professor O. T. Beachley<br>Department of Chemistry<br>State University of New York<br>Buffalo, New York 14214 | 1 |
| Professor P. S. Skell<br>Department of Chemistry<br>The Pennsylvania State University<br>University Park, Pennsylvania 16802 | 1 |
| Professor K. M. Nicholas<br>Department of Chemistry<br>Boston College<br>Chestnut Hill, Massachusetts 02167 | 1 |

# TECHNICAL REPORT DISTRIBUTION LIST, GEN

| | No. Copies |
|---|---|
| Office of Naval Research<br>800 North Quincy Street<br>Arlington, Virginia 22217<br>Attn: Code 472 | 2 |
| ONR Branch Office<br>536 S. Clark Street<br>Chicago, Illinois 60605<br>Attn: Dr. George Sandoz | 1 |
| ONR Branch Office<br>715 Broadway<br>New York, New York 10003<br>Attn: Scientific Dept. | 1 |
| ONR Branch Office<br>1030 East Green Street<br>Pasadena, California 91106<br>Attn: Dr. R. J. Marcus | 1 |
| ONR Area Office<br>One Hallidie Plaza, Suite 601<br>San Francisco, California 94102<br>Attn: Dr. P. A. Miller | 1 |
| ONR Branch Office<br>Building 114, Section D<br>666 Summer Street<br>Boston, Massachusetts 02210<br>Attn: Dr. L. H. Peebles | 1 |
| Director, Naval Research Laboratory<br>Washington, D. C. 20390<br>Attn: Code 6100 | 1 |
| The Assistant Secretary<br>of the Navy (R,E&S)<br>Department of the Navy<br>Room 4E736, Pentagon<br>Washington, D. C. 20350 | 1 |
| Commander, Naval Air Systems Command<br>Department of the Navy<br>Washington, D. C. 20360<br>Attn: Code 310C (H. Rosenwasser) | 1 |
| Defense Documentation Center<br>Building 5, Cameron Station<br>Alexandria, Virginia 22314 | 12 |
| U. S. Army Research Office<br>P. O. Box 1211<br>Research Triangle Park, N.C. 27709<br>Attn: CRD-AA-IP | 1 |
| Naval Ocean Systems Center<br>San Diego, California 92152<br>Attn: Mr. Joe McCartney | 1 |
| Naval Weapons Center<br>China Lake, California 93555<br>Attn: Dr. A. B. Amster<br>Chemistry Division | 1 |
| Naval Civil Engineering Laboratory<br>Port Hueneme, California 93401<br>Attn: Dr. R. W. Drisko | 1 |
| Professor K. E. Woehler<br>Department of Physics & Chemistry<br>Naval Postgraduate School<br>Monterey, California 93940 | 1 |
| Dr. A. L. Slafkosky<br>Scientific Advisor<br>Commandant of the Marine Corps<br>(Code RD-1)<br>Washington, D. C. 20380 | 1 |
| Office of Naval Research<br>800 N. Quincy Street<br>Arlington, Virginia 22217<br>Attn: Dr. Richard S. Miller | 1 |
| Naval Ship Research and Development<br>Center<br>Annapolis, Maryland 21401<br>Attn: Dr. G. Bosmajian<br>Applied Chemistry Division | 1 |
| Naval Ocean Systems Center<br>San Diego, California 91232<br>Attn: Dr. S. Yamamoto, Marine<br>Sciences Division | 1 |